Journal of Nuclear Materials 390–391 (2009) 207–210

Contents lists available at ScienceDirect

Journal of Nuclear Materials

journal homepage: www.elsevier.com/locate/jnucmat

Coupled IMPGYRO-EDDY simulation of tungsten impurity transport in tokamak geometry

M. Toma [a,*], K. Hoshino [b], K. Inai [c], M. Furubayashi [a], A. Hatayama [a], K. Ohya [c]

[a] Faculty of Science and Technology, Keio University, 3-14-1 Hiyoshi, Kouhoku, Yokohama 223-8522, Japan
[b] Naka Fusion Institute, Japan Atomic Energy Agency, 311-0193, Japan
[c] Institute of Technology and Science, The University of Tokushima, 770, Japan

ARTICLE INFO

PACS:
52.55.Fa
52.25.Vy
52.25.Fi
52.40.Hf

ABSTRACT

We are developing a Monte Carlo transport code, 'IMPGYRO' for high-*Z* impurities. The code includes most of important process of high-*Z* impurities: (1) the finite Larmor radius effect in realistic tokamak geometries, (2) Coulomb collision of impurity ions with background ions and (3) multi-step ionization/recombination process. In this study, the IMPGYRO code is coupled to the EDDY code to improve the impurity generation model. The coupled code has been applied to the analysis of tungsten in a typical detachment state and has output the initial results. The code more precisely takes into account the effect of re-emission (reflection and self-sputtering). The resultant density inside the core becomes about two times larger than that with the previous simple impurity generation model. These initial results show that the coupling the IMPGYRO-EDDY code makes it possible to analyze not only the large-scale transport process of high-*Z* impurities in a realistic tokamak geometry, but also their re-emission process on the material surface more correctly.

1. Introduction

Recently, tungsten has been paid attention as a divertor material that is not subjected to chemical sputtering. The radiation-cooling problem of core plasma, however, might arise even if a small amount of such a high-*Z* impurity enters the core plasma region. Therefore, it is very important to understand the transport process of tungsten impurities in the plasma region and to evaluate the amount of impurities that enter the core plasma.

For this purpose, we are developing the IMPGYRO code [1–3]. The code numerically follows trajectories of impurity test neutrals/ions in realistic tokamak geometries. Their Larmor gyro-motions are directly taken into account without the guiding-center approximation. Important elastic/inelastic collisions with background plasma are included by the Monte Carlo method. The tungsten atomic data [4] are used for ionization/recombination. As for the impurity generation process, however, a relatively simple model was employed. The simple analytic formulae [5–7] were used for the sputtering yield, angular and energy distribution of sputtered ions in the previous version of IMPGYRO code. In this study, the IMPGYRO code is coupled to the EDDY (Erosion and Deposition based on DYnamic model) code [8] in order to improve the impurity generation model.

2. Code improvement and calculation conditions

As mentioned above, the IMPGYRO code is coupled to the EDDY code in the present study. The EDDY code simulates the slowing down of incident ions in the material and formation of recoil cascades leading to processes such as ion reflection and physical sputtering [8]. In addition, the following improvements have been done: (1) to speed up the calculation, the code is parallelized and its optimization has been done, (2) the code is improved to calculate the time-dependent/dynamic behavior of the impurity transport, and (3) the effect of the sheath is taken into account [9].

The model geometry and numerical mesh used in the present calculation are shown in Fig. 1, which are generated from a JT-60U MHD equilibrium. The background plasma profiles are calculated by the SOL/divertor plasma-simulation code, the B2.5-EIRINE code [10]. Fig. 2 shows the background plasma profiles of electron density and temperature. The bulk ion density at the core interface is fixed to $n_D = 2.8 \times 10^{19}$ m^{-3} and the background divertor plasma is in a typical power detachment state. In this initial calculation after the coupling to the EDDY code, we focus the effect of re-emission (self-sputtering and reflection) process and a relatively simple setup has been adopted for the primary impurity, i.e., the first generation of impurities: 40 test particles per every 100 time-steps are uniformly launched from the divertor plate as a neutral tungsten particle monoenergetic of 10 eV with a cosine angular distribution. Also, the relatively simple assumption has been made for the

* Corresponding author.
E-mail address: toma@ppl.appi.keio.ac.jp (M. Toma).

0022-3115/$ - see front matter © 2009 Elsevier B.V. All rights reserved.
doi:10.1016/j.jnucmat.2009.01.169

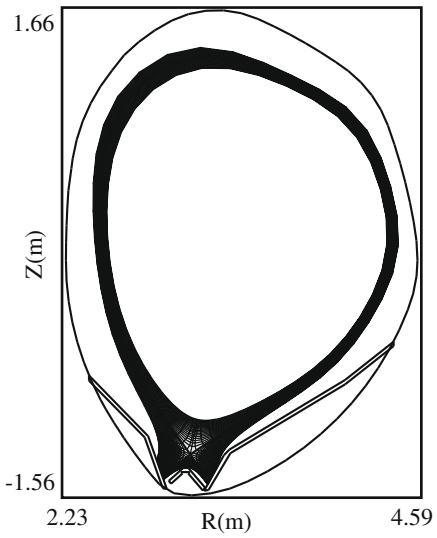

Fig. 1. Model geometry and numerical mesh.

boundary condition. Re-emission process takes place only on the divertor plates. If test particles reach other boundaries in Fig. 1, test particles are assumed to be absorbed (no reflection/self-sputtering). The two cases have been calculated: (a) with the coupled IMPGYRO-EDDY model and (b) with the previous Simple Analytic formulae. Hereafter, the abbreviations CE and SA will be used for the former and the latter model. Notice that the CE model takes into account both self-sputtering and reflection as the re-emission process, however, the SA model takes into account only the self-sputtering. The details of the SA model are given in the previous study in Ref. [3].

3. Results and discussion

Fig. 3 shows the time evolution of the total number of impurity particles in the core. In Fig. 3, the time evolutions are compared for the two different model, i.e., (1) the present CE model and the previous SA model. The 2D impurity density profiles near the X-point are compared in Fig. 4. As seen from Fig. 4(a) and (b), qualitatively, the spatial profiles with the CE and SA model are similar. The total number inside the core region, however, is about two times larger with the CE model than that with the SA model.

To understand the difference, Table 1 summarizes the number of the surface re-emission process observed in the calculations shown in Fig. 3. As shown in Table 1, the number of self-sputtered particles is very small in both cases. On the other hand, the number

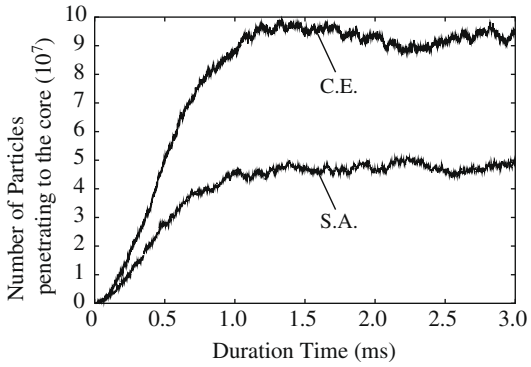

Fig. 3. Time evolutions of the total number of test impurity particles in the core region (between the core interface boundary and the separatrix) are compared: (a) with the coupled IMPGYRO-EDDY (CE) model and (b) with the previous simple analytic (SA) model.

of the reflected particles is about 96% of the total number of incident particles with the C.E. model. This large fraction of reflected particles at the divertor plate leads to the increase in the impurity density penetrating into the core region with the CE model in Fig. 3.

The reason why the reflection process dominates the surface process can be explained by the angular and the energy distribution of the incident particles. Fig. 5 shows distribution of the incident angle of the particles that hit the divertor plate during the time-evolution in Fig. 3. In this initial calculation, we have applied the IMPGYRO code to the typical detached state. The incident energies of impurities are relatively low. Fig. 6 shows the dependence of the surface re-emission yield on the incident angle calculated from the EDDY code. As seen from Fig. 6, reflection coefficients obtained from the EDDY become considerably large in the range of the incident angle 60–90°. This angular dependence of re-emission yield, together with the angular distribution obtained in the simulation (Fig. 5), explains the results in Table 1.

As was shown in Table 1, the total re-emission yield at the divertor plate calculated from the CE model is about 30 times larger than that from the SA model. However, the number of the impurity particles in the core with the CE model in Fig. 3 is only about two times larger than with the SA model. To understand this feature, the following simple global particle-balance model is useful.

The total number of the impurity particles N_T in the system for the steady state can be estimated by the equation, $N_T = S\tau_p^*$, where S is the primary impurity source. The effective confinement time τ_p^* of impurity particles including the effect of particle re-emission at the divertor plate is given by $\tau_p^* = \tau_p/(1 - R_{eff})$, where τ_p^* is the intrinsic particle confinement time without the effect of re-emission and R_{eff} is the effective recycling (re-emission) coefficient.

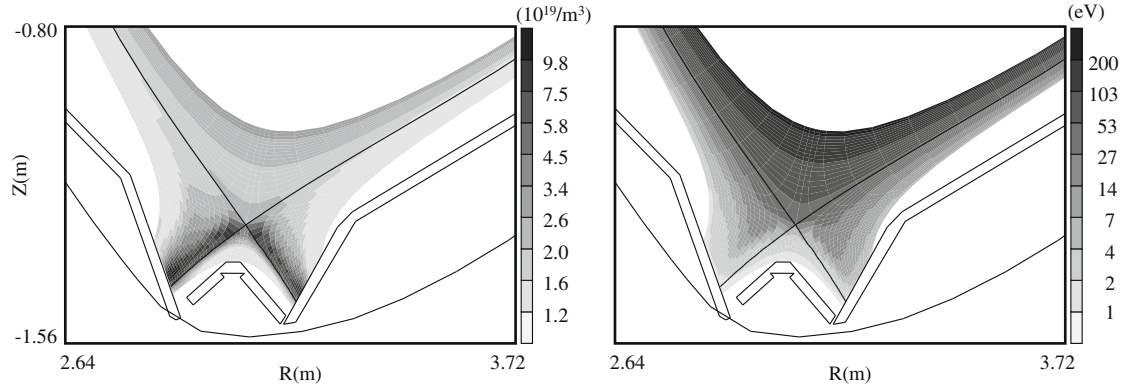

Fig. 2. Background plasma profiles (a) electron density and (b) electron temperature. Zoom in view near the divertor region in Fig. 1.

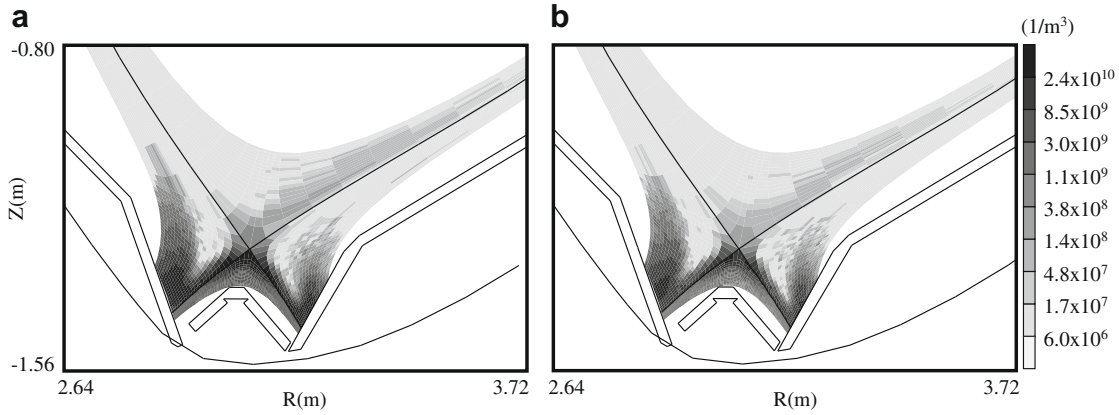

Fig. 4. Two-dimensional spatial profiles of impurity density (the sum of the each charge state): (a) with coupled IMPGYRO-EDDY model and (b) with the simple analytic model. The profile are plotted using the time-averaged value at each cell during the quasi-steady state in Fig. 3.

Table 1
Sputter yield and reflection coefficient at the divetror plate. The sputter yield is defined by $Y_{SP} = N_{SP}/N_{TD}$, while the reflection coefficient is by $Y_{RF} = Y_{RF}/N_{TD}$ N_{SP} and N_{RF} are the total number of sputtered particle and reflected particles at the divertor plate, respectively, while N_{TD} is the total number of impurity reaching the divertor plate during the quasi-steady state in Fig. 3. The re-emission yield is given by $\gamma = Y_{SP} + Y_{RF}$.

	Sputter yield Y_{SP} (%)	Reflection coefficient Y_{RF} (%)	Re-emission yield $\gamma = Y_{SP} + Y_{RF}$ (%)
CE	0.2	96.2	96.4
SA	3.1	–	3.1

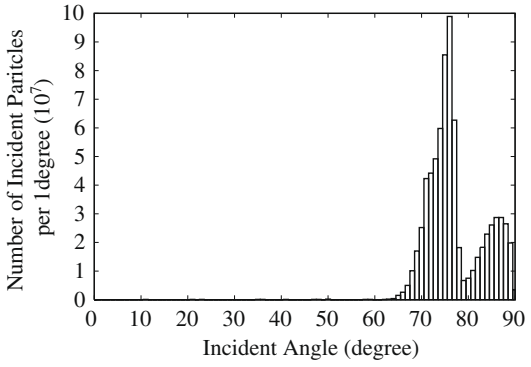

Fig. 5. Angular distribution of incident impurity particles to the divertor plate during the quasi-steady state in Fig. 3.

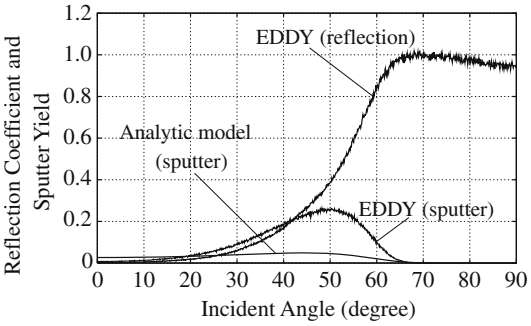

Fig. 6. Re-emission yield (self-sputter yield and reflection coefficient) calculated by the EDDY code. The incident energy is fixed at 100 eV and 10^4 test incident particles are used to obtain the yield for each incident angle in this EDDY stand-alone calculation. The sputter yield from the analytic model is also plotted.

Table 2
The number of impurity particles reaching each calculation boundary. The number is normalized by the total numbers of impurity particles reaching all the boundaries (see Fig. 1) during the quasi-steady state in Fig. 3.

	Inner divertor (%)	Outer divertor (%)	Dome (%)	First wall (%)	Core interface (%)
CE	20.0	46.2	32.7	1.1	~0
SA	26.1	38.8	33.6	1.5	~0

The source S for the CE and the SA are the same, because injection rates of the primary impurity are the same as mentioned in Section 2. Therefore, the ratio of the total number of the impurity in the system becomes as $N_T^{CE}/N_T^{SA} = \tau^*_{p,CE}/\tau^*_{p,SA}$. To calculate this ratio, it is necessary to estimate τ^*_p, i.e., τ_p and R_{eff} for both models. The intrinsic confinement time τ_p can be obtained as follows. After the system reaching the quasi-steady state, we stop injecting the primary impurity and set all the calculation boundaries as absorbing boundaries. Then, the number of the impurity in the system starts decreasing. From this time-decay of N_T, τ_p with the CE and the SA are estimated to be $\tau_{p,CE} = \tau_{p,SA} = 0.27$ ms. They are almost the same as expected, while the re-emission yield γ at the divertor plate largely depends on the model (Table 1: $\gamma^{CE} = 0.96$ and $\gamma^{SA} = 0.03$. For the calculation of R_{eff}, it should be noted that $R_{\mathrm{eff}} \neq \gamma$, because the divertor plate is assumed to be the only re-emission boundary and the remaining boundaries are assumed to be the absorbing boundaries. Therefore, R_{eff} may be written as $R_{\mathrm{eff}} = A_{\mathrm{eff}}\gamma$, where A_{eff} is the 'effective' ratio of the divertor surface-area to the total surface-area. Table 2 shows the number of impurity particles reaching each calculation boundary. From Table 2, the effective surface-ratio of the divertor plate becomes $A_{\mathrm{eff}}^{\mathrm{CE}} = 0.66$ and $A_{\mathrm{eff}}^{\mathrm{SA}} = 0.65$, respectively. From these values, we finally obtain the ratio as $N_T^{\mathrm{CE}}/N_T^{\mathrm{SA}} = 2.7$, which reasonably agrees with the simulation result shown in Fig. 3.

4. Conclusion and outlook

Above initial results show the importance of IMPGYRO-EDDY coupling. The coupling makes it possible to analyze, not only the large spatial-scale transport process of impurities in realistic geometry of tokamaks, but also surface-interaction process near the divertor plate more accurately. The code, however, is still under the development and the following improvements will be needed for the final goal of the IMPGYRO code development, i.e., to develop the simulation code for the reliable and precise prediction of the impurity behavior in the future fusion reactors: (1) implement

the radiation model and evaluate not only the impurity density, but also the radiation power and its effects on the background plasma, (2) implement the atomic data for the carbon impurity and simulate the co-existing system of W and C, (3) Coupling to the SOL/Divertor code for the background plasma and more self-consistent simulation, and (4) detailed code validation against the experimental results.

Acknowledgement

This study is partially supported by a Grant-in-Aid for Scientific Research of the Japan Society for the Promotion of Science.

References

[1] I. Hyodo et al., J. Nucl. Mater. 313–316 (2003) 1183.
[2] A. Fukano et al., J. Nucl. Mater. 363–365 (2007) 211.
[3] K. Hoshino et al., Contrib. Plasma Phys. 48 (2008) 280.
[4] K. Asmussen et al., Nucl. Fus. 38 (7) (1998) 967.
[5] J. Roth, Physical sputtering of solids at ion bombardment, in: D.E. Post, R. Behrisch (Eds.), Physics of Plasma–Wall Interactions in Controlled Fusion, Plenum, New York, 1984, pp. 351–388.
[6] Y. Yamamura et al., Nagoya University, Japan Report IPPJ-AM-26.
[7] M.W. Thompson, Philos. Mag. 18 (1968) 377.
[8] K. Ohya, Phys. Scr. T124 (2006) 70.
[9] K. Hoshino et al., J. Nucl. Mater. 390–391 (2009) 168.
[10] R. Schneider et al., Contrib. Plasma Phys. 46 (2006) 3.